Optimum Static Balancing of the Parallel Robot for Medical 3D-Ultrasound Imaging

S. Lessard*, P. Bigras, I. A. Bonev

Département de génie de la production automatisée
École de Technologie Supérieure (ETS)
1100 Notre-Dame St. W, Montréal, QC
Canada, H3C 1K3

S. Briot, V. Arakelian

Département de Génie Mécanique et Automatique,
L.G.C.G.M. – EA3913
Institut National des Sciences Appliquées (I.N.S.A.)
20 Buttes de Coësmes Av. – CS 14315
F-35043 Rennes, France

Abstract - *Static balancing of mechanical systems is useful and required in many situations. The objective of such balancing is the compensation of gravitational forces in order to achieve a static equilibrium. A balanced system becomes safer and actuators are reduced in size. However, balancing a system requires numerous complex mechanical add-ons or unavoidable addition of mass. This is the reason why methods of partial static balancing have been developed and applied in practice. In this paper, a newly designed parallel robot for medical 3D-ultrasound imaging is required to be statically balanced without complicated design modifications. Simple mechanical add-on that is optimally designed can reduce substantially the effect of gravity. The efficiency of these suggested solutions is illustrated by numerical simulation of the robot.*

Keywords: static equilibrium, parallel robot, medical robot, root-mean-square minimization

I. Introduction

Recently, parallel robotics has broken through new field of research such as high speed manipulation, material handling, motion platforms and medical equipment. In the latter, a new robot has been developed at *École de technologie supérieure* (Fig. 1). This robot is designed to perform an ultrasound scan of a human patient's arteries. It consists of two five-bar planar mechanisms, which are connected to a tool holder by an articulated telescopic strut. Four motors are mounted inside the main frame while a fifth motor is attached directly to the tool holder allowing large amplitude tool rotations. The whole frame is mounted on a linear motor which allows large horizontal displacements of the robot. Thus, such an architecture has six degrees of freedom and ensures the required geometric and kinematic characteristics (see tables I and II) [1].

The robot workspace was defined considering the examination of one half of the human body, cut vertically (Fig. 2). A robot suited for the quantification of the lower limbs arteries could perform any less restricting arterial examination since it is the longest arterial examination. The linear displacement was chosen long enough to cover the whole body from neck down, thus preventing repositioning of the patient for different examinations or having to place him meticulously in the robot workspace. Designing a robot for a precise confined workspace would have led to a less practical system.

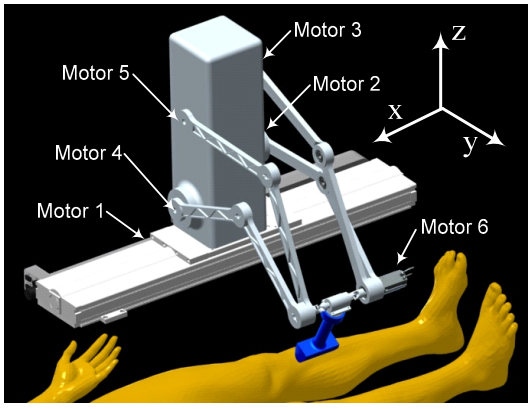

Fig. 1. CAD model of the prototype parallel robot

Axis	Dimension (mm)	Description
X	1500	Span (arteries axis)
Y	500	Lateral
Z	500	Vertical

TABLE I. Positioning workspace dimensions

Axis	Orientation (degree)	Description
Around X	-75° to 90°	Span (arteries axis)
Around Y	-50° to 35°	Lateral
Around Z	-45° to 45°	Vertical

TABLE II. Workspace orientations

* E-mail: simon.lessard.3@ens.etsmtl.ca
A partnership with *Institut National des Sciences Appliquées* (Rennes, France) has led to this present work on optimum static balancing of the six-degree-of-freedom medical robot.

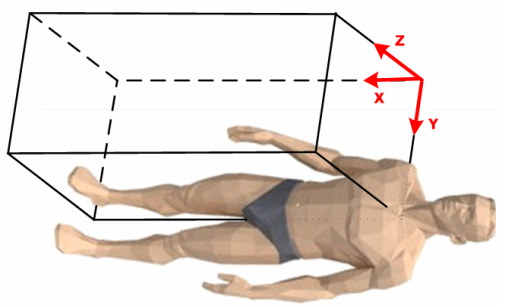

Fig. 2. Required workspace for the robotized ultrasound examination

The first virtual prototype version of the robot (Fig. 1) is smaller resulting in a smaller workspace. For assembly considerations, symmetric motors of each five-bar mechanism are not mounted *vis-à-vis*.

The robot design next step is the minimization of the input torques. This goal is well-known in the field of robotics and is composed of the static balancing of moving masses.

Static balancing is typically achieved by adding a counterweight or a spring to each bar. Complete static balancing is carried out by keeping constant the potential energy of the system for all configurations. In previous studies, a number of methods have been proposed for gravity balancing of robotic systems: spring balancing of a planar pantograph [2, 3], n-springs solutions to a single attached point [4], balancing of a spatial positioning table [5] and 6-dof parallel manipulators [6, 7], as well as several auxiliary mechanisms for spring support [8-12].

This article deals with the optimum static balancing of a parallel robot developed for medical 3D-ultrasound imaging. The suggested analytical solution allows a significant reduction in the input torques by means of simpler design solutions. The paper is organized as follows. Firstly, the input torques due to the static and dynamic loads are examined and a simplified calculation approach is proposed. Then an optimal static balancing method is developed, which is formulated by the input torques root-mean-square values minimization.

II. Static and Dynamic Models

In our medical robotic application, motion is slow and smooth. Therefore, the end-effector velocity and acceleration are small. Our observations show that the input torques caused by the inertia effect of the moving masses are very small compared to the input torques caused by the gravity force. Thus, inertia effect can be neglected. For example, the variation of the input torques for a prescribed trajectory (with 0.6m/s^2 maximal acceleration) shows that the maximal difference between the dynamic and the static loads is less than 1%. This means that the motor torques are mainly caused by gravity.

III. Complete Static Balance

Counterweights mounted on each moving links achieve complete static equilibrium. Fig. 3 illustrates the complete static balance of the parallel robot for medical 3D-ultrasound.

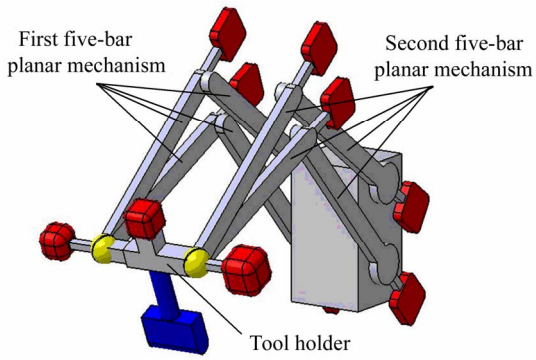

Fig. 3. Complete balancing by counterweights

Clearly, the added counterweights increase the robot's inertia. Also, the tool holder motor would be difficult to assemble with a counterweight attached because the joint is not a ball joint, but a combination of a universal joint and a revolute joint.

In the case of complete balancing with springs, it is necessary to add auxiliary mechanisms (parallelograms), which lead to a very complicated mechanical architecture.

A mechanical system that is completely balanced becomes either very heavy or too complicated to manufacture and assemble. That is why we developed a partial balancing approach. It is obvious that the load reduction on actuators is partial, but the design solution is very simple.

IV. Input Torques

The input torque of the ith actuator can be expressed as:

$$\tau_i = \sum_{j=1}^{13} \left(\mathbf{J}_j^T \right)_i \cdot \mathbf{G}_j \qquad (i = 1,...,6) \qquad (1)$$

where $(\mathbf{J}^T_j)_i$ corresponds to the ith line of the transposed Jacobian matrix between the center of masses S_j of the link j and the actuated variables q_i. $\mathbf{G}_j$ is the gravity forces of the link j (Fig. 4-6).

The structure of this robot has some particularities which allow a considerable simplification of torques determination. The tool holder represents an Assur group [13] with two links and three joints (spherical, universal and revolute pairs) dividing the robot architecture in two parts. Thus the tool holder can be disconnected from the robot structure to be examined separately.

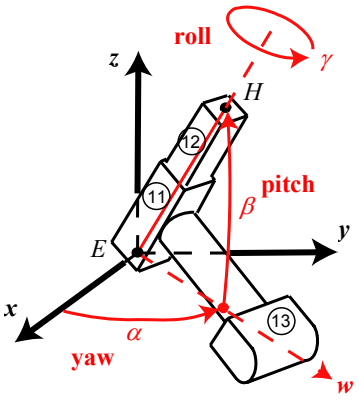

Fig. 4. Euler angles of the tool

From this point forward, the tool is considered statically balanced around the sixth motor, i.e. the tool's center of mass coincides with the motor rotation axis. Such an approach simplifies reaction forces and input torques calculations.

The reaction forces R_E and R_H (respectively applied by the tool holder at points E and H) are function of the yaw and pitch angles only, the roll angle being equal to the sixth motor rotation angle, this motor input torque being independent of the other motors.

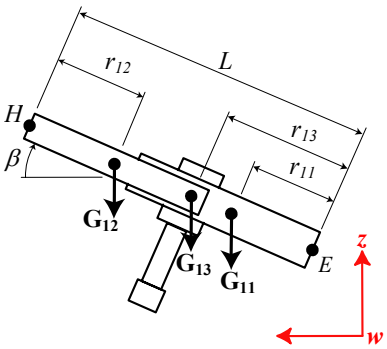

Fig. 5. Schematic of the tool assembly

The length L of the passive linear joint is calculated as a function of the orientation angles:

$$L = L_f \frac{\cos\beta}{\cos\alpha} \tag{2}$$

where L_f is the distance between the two planar five bar mechanisms: $L_f = |x_E - x_H|$.

Thus, the vertical reaction forces on point H and E can be determined from the static equilibrium equations:

$$R_{Hz} = \frac{(m_{12}(L - r_{12}) + m_{11}r_{11} + m_{13}r_{13})g}{L} \tag{3}$$

$$R_{Ez} = (m_6 + m_{11} + m_{12} + m_{13})g - R_{Hz} \tag{4}$$

where m_i, and r_i are respectively the mass and position of the centre of masses of the i[th] link, g is the gravity and m_6 is the mass of actuator 6.

The horizontal reaction forces are projected from axis ***w*** to axis ***y***:

$$R_{Hy} = (m_{12}g - R_{Hz})\tan\beta\sin\alpha \tag{5}$$

$$R_{Ey} = -R_{Hy} \tag{6}$$

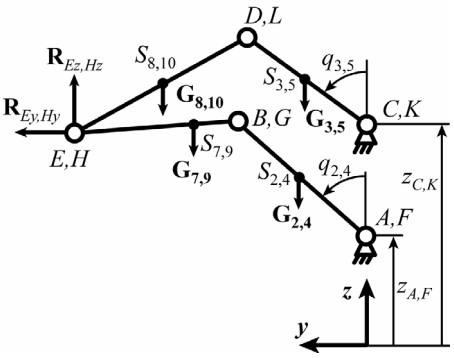

Fig. 6. Schematics of the two five-bars mechanisms with applied reaction forces

Thus, it is possible to deduce the potential energy V of the first five bar mechanism (Fig. 6):

$$V = (m_2 z_2 + m_3 z_3 + m_7 z_7 + m_8 z_8)g + R_{Ez} z_E + R_{Ey} y_E \tag{7}$$

with

$$z_2 = z_A + r_2 \cos q_2 \tag{8}$$

$$z_3 = z_C + r_3 \cos q_3 \tag{9}$$

$$z_7 = (L_2 \cos q_2 + z_A - z_E)\frac{r_7}{L_7} + z_E \tag{10}$$

$$z_8 = (L_3 \cos q_3 + z_C - z_E)\frac{r_8}{L_8} + z_E \tag{11}$$

where z_i is the vertical coordinate of the centre of mass S_i of the i[th] link and r_2=AS_2, r_3=CS_3, r_7=ES_7, r_8= ES_8.

Then the input torques are determined by differentiating the potential energy by the motor articulation position vector $\mathbf{Q}$. To transform the reaction forces at the tip into reaction motor torques, a Jacobian matrix is needed [14]:

$$\boldsymbol{\tau} = \begin{bmatrix} \tau_2 \\ \tau_3 \end{bmatrix} = \frac{\partial V}{\partial \mathbf{Q}} - \mathbf{J}^T \frac{\partial V}{\partial \mathbf{E}} \tag{12}$$

where τ_i is the i[th] actuator torque, $\mathbf{Q} = [q_2, q_3]$ and $\mathbf{J}$ is the five-bar mechanism's Jacobian matrix [15]. The obtained expression of $\boldsymbol{\tau}$ is given in appendix 1.

The second five-bar mechanism's torques τ_4 and τ_5 of actuators 4 and 5 are determined in a similar way.

V. Input Torques Root-Mean-Square Values Minimization

The input torques minimization is carried out by each actuator torque root-mean-square values minimization for all the workspace. The workspace used in the calculation is only the ***yz*** plane because the linear motorized axis is not subject to gravity balancing. Three solutions are considered for optimum balancing.

A. Tension / Compression Spring Equilibrium

Firstly, one solution is an equilibrium mechanical system composed of zero free length springs (tension or compression) attached on each motorized arms. The fixed end of each spring is positioned optimally to release the actuator.

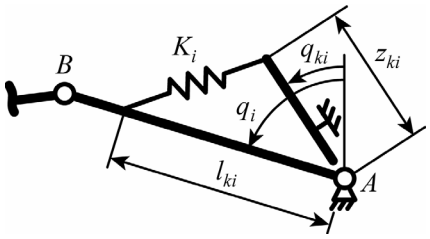

Fig. 7. Spring balancing

The spring applied torque's potential energy is:

$$V_{ki} = \frac{K_i}{2}[(z_{ki}\cos q_{ki} - l_{ki}\cos q_i)^2 + (z_{ki}\sin q_{ki} - l_{ki}\sin q_i)^2] \quad (13)$$

where K_i is the stiffness spring coefficient, which is attached on a fixed arm of length z_{ki} and orientation q_{ki} (Fig.7) and q_i is the angular position of the i^{th} actuator. The other end is linked on the motorized arm at length l_{ki}.

By differentiating equation (13), we determine the input torque:

$$\tau_{ki} = \frac{\partial V_{ki}}{\partial q_i} = K_i\, l_{ki}\, z_{ki} \sin(q_i - q_{ki}) \quad (14)$$

The spring stiffness coefficient K_i and attached linear positions z_{ki} and l_{ki} are consolidated into parameter C_i. Thus, the optimal calculated C_i will position precisely a certain spring K_i on the arms:

$$\tau_{ki} = C_i \sin(q_i - q_{ki}) \quad (15)$$

Two parameters have to be optimized for each motor: the constant C_i and the angular position of the fixed arm q_{ki}.

The torque root-mean-square value minimization leads to the following condition:

$$f_i = \sum_{WS}(\tau_i + \tau_{ki})^2 \rightarrow \min_{C_i, q_{ki}} \quad (i=2,\ldots,5) \quad (16)$$

where WS := Workspace. For this purpose, these conditions must be satisfied:

$$\frac{\partial f_i}{\partial C_i} = 0 \text{ and } \frac{\partial f_i}{\partial q_{ki}} = 0 \quad (17)$$

from which the coefficients are solved:

$$q_{ki} = 2\arctan(t_{mi}) \quad (m=1,\ldots,6) \quad (18)$$

$$C_i = \frac{-\sum_{WS}\tau_i \sin(q_i - q_{ki})}{\sum_{WS}\sin^2(q_i - q_{ki})} \quad (19)$$

where t_{mi} are the roots of a polynomial $p_i(t)$ given in appendix 2.

B. Torsion Spring Equilibrium

Secondly, static balance can be achieved using torsion spring mounted on each actuator axes. The spring torque is linear to the bending angle:

$$\tau_{ki} = K(q_{ki} - q_i) \quad (20)$$

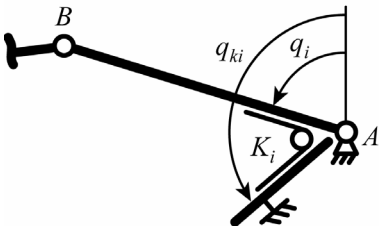

Fig. 8. Torsion spring balancing

The minimization conditions are the same:

$$f_i = \sum_{WS}(\tau_i + \tau_{ki})^2 \rightarrow \min_{K_i, q_{ki}} \quad (i=2,\ldots,5) \quad (21)$$

$$\frac{\partial f_i}{\partial K_i} = 0 \text{ and } \frac{\partial f_i}{\partial q_{ki}} = 0 \quad (22)$$

from which the coefficients are solved:

$$q_{ki} = \frac{\sum_{WS}\tau_i q_i \sum_{WS} q_i - \sum_{WS}\tau_i \sum_{WS} q_i^2}{N\sum_{WS}\tau_i q_i - \sum_{WS}\tau_i \sum_{WS} q_i} \quad (23)$$

$$K_i = -\frac{\sum_{WS}\tau_i (q_{ki} - q_i)}{\sum_{WS}(q_{ki} - q_i)^2} \quad (24)$$

where N is the number of calculated positions in the workspace.

C. Counterweight Equilibrium

Lastly, a balancing approach is carried out by adding a counterweight of mass M_i on each motorized axis.

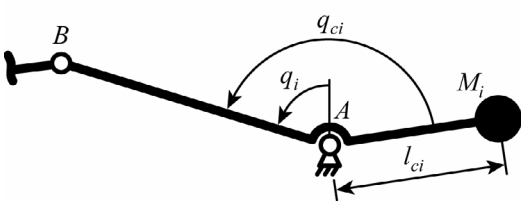

Fig. 9. Counterweight balancing

The mass M_i is placed at a certain angle so that the maximum torque applied is at a specific desired motor angle. The optimum counterweight system is then function of the mass M_i and position q_{ci} for a given length l_{ci}.

$$\tau_{ci} = -M_i l_{ci} \sin(q_i - q_{ci}) \tag{25}$$

The mass M_i and length l_{ci} are consolidated into a single constant C_i:

$$\tau_{ci} = -C_i \sin(q_i - q_{ci}) \tag{26}$$

Determination of parameters C_i and q_{ci} is equivalent to the determination of parameters C_i and q_{ki} in section *A*.

VI. Results

The proposed robot (Fig. 1) with above mentioned geometrical parameters and mass distribution (appendix 3) was used for numerical simulation. Three mechanical solutions were tested. As a mean of comparison, reductions of the RMS and maximum motor torques are given in tables (III)-(V).

Motor	Tension/Compression spring Parameters		RMS	Max Torque
2	q_{k2} = 1.7°	C_2 = 0.104 Nm	57.6%	34.7%
3	q_{k3} = -42.7°	C_3 = 0.263 Nm	91.2%	45.6%
4	q_{k4} = 3.4°	C_4 = 0.081 Nm	50.1%	33.1%
5	q_{k5} = -43.0°	C_5 = 0.187 Nm	90.2%	43.1%

TABLE III. Tension / compression spring optimum configurations

Motor	Torsion spring Parameters		RMS	Max Torque
2	q_{k2} = 7.7°	K_2 = -4.55 Nm/rad	56.9%	45.4%
3	q_{k3} = 180°	K_3 = 5.29 Nm/rad	90.4%	45.2%
4	q_{k4} = 6.2°	K_4 = -3.33 Nm/rad	50.0%	46.7%
5	q_{k5} = 180°	K_5 = 3.74 Nm/rad	89.2%	34.3%

TABLE IV. Torsion spring optimum configurations

Motor	Counterweight Parameters		RMS	Max Torque
2	q_{c2} = -178.4°	C_2 = 4.63 Nm	57.6%	34.7%
3	q_{c3} = -221.4°	C_3 = 11.63 Nm	91.5%	46.4%
4	q_{c4} = -176.9°	C_4 = 3.62 Nm	50.1%	33.1%
5	q_{c5} = -224.2°	C_5 = 8.36 Nm	90.2%	44.1%

TABLE V. Counterweight optimum configurations

The static torque root-mean-square sum minimization was reduced up to 50% ÷ 91.5%. In more practical terms, the maximum motor torque required was reduced up to 34.3% ÷ 46.7% .

Fig. 10 shows input torques variations for unbalanced and optimum balanced robots with extension springs (the simulation was carried out in a static mode or operation).

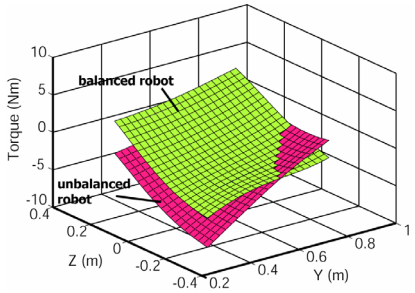

(a) Actuator 2

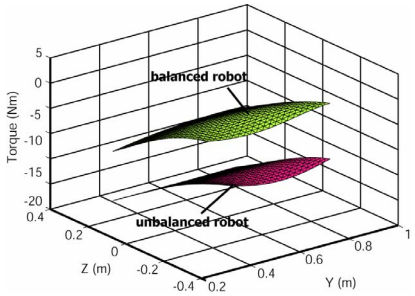

(b) Actuator 3

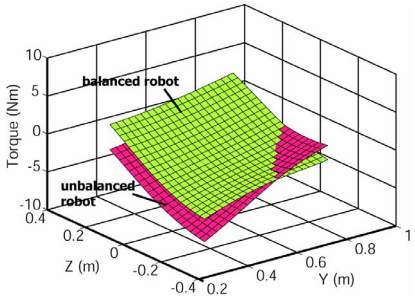

(c) Actuator 4

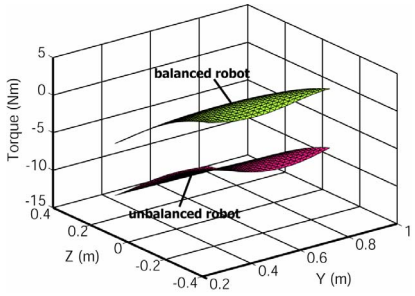

(d) Actuator 5

Fig. 10. Variation of the actuator torques for the orientation angles α=β=γ=0 deg

VII. Conclusion

The perfect static balancing of a spatial multibody mechanical system can eliminate completely the load caused by the gravity force. However, such a solution leads to inevitably complicated design add-ons or to unavoidable increase in total mass. In most cases, the complete balance is achieved only in theory but not in practice. In this paper, a parallel robot for medical 3D-ultrasound imaging was optimally statically balanced. The proposed simple solutions presented a partial balancing effect minimizing the actuator torques.

Future work will investigate more efficient minimization by increasing the number of variables to the problem. The development of a prototype with the suggested balancing system is planned.

References

[1] S. Lessard, I. Bonev, P. Bigras, L.-G. Durand, G. Soulez, G. Cloutier, and J. A. DeGuise, "Parallel Robot for Medical 3D-Ultrasound Imaging," presented at International Symposium on Industrial Electronics, École de technologie supérieure, Montréal, Canada, 2006.

[2] J. L. Herder, "Energy-Free Systems. Theory, conception and design of statically balanced mechanisms", PhD Thesis: Delf University of Technology, 2001.

[3] E. Shin and D. A. Streit, "Spring equilibrator theory for static balancing of planar pantograph linkages," *Mechanism & Machine Theory*, vol. 26, pp. 645-657, 1991.

[4] G. J. Walsh, D. A. Streit, and B. J. Gilmore, "Spatial spring equilibrator theory," *Mechanism & Machine Theory*, vol. 26, pp. 155-170, 1991.

[5] J. Wang and C. M. Gosselin, "Static balancing of spatial three-degree-of-freedom parallel mechanisms," *Mechanism & Machine Theory*, vol. 34, pp. 437-452, 1999.

[6] I. Ebert-Uphoff, C. M. Gosselin, and T. Laliberte, "Static balancing of spatial parallel platform mechanisms - revisited," *Journal of Mechanical Design, Trans. of the ASME*, vol. 122, pp. 43-51, 2000.

[7] C. M. Gosselin and J. Wang, "Static balancing of spatial six-degree-of-freedom parallel mechanisms with revolute actuators," *Journal of Robotic Systems*, vol. 17, pp. 159-170, 2000.

[8] A. Fattah and S. K. Agrawal, "On the design of a passive orthosis to gravity balance human legs," *Journal of Mechanical Design, Transactions of the ASME*, vol. 127, pp. 802-808, 2005.

[9] A. Fattah and S. K. Agrawal, "Gravity-Balancing of Classes of Industrial Robots," presented at International Conference on Robotics and Automatics, Orlando, Florida, 2006.

[10] I. Simionescu and L. Ciupitu, "Static balancing of the industrial robot arms. Part I: discrete balancing," *Mechanism and Machine Theory*, vol. 35, pp. 1287-1298, 2000.

[11] I. Simionescu and L. Ciupitu, "Static balancing of the industrial robot arms. Part II: continuous balancing," *Mechanism and Machine Theory*, vol. 35, pp. 1299-1311, 2000.

[12] J. Wang and C. M. Gosselin, "Passive mechanisms with multiple equilibrium configurations," *Transactions of the Canadian Society for Mechanical Engineering*, vol. 28, pp. 139-151, 2004.

[13] V. Zinoviev, *Théorie des mécanismes et des machines,* Ed. de la Paix (Moscou), 215p., 1975.

[14] R. Clavel and K. Miller, "The Lagrange-Based Model of Delta-4 Robot Dynamics," *Robotersysteme*, vol. 8, pp. 49-54, 1992.

[15] C. Gosselin and J. Angeles, "Singularity analysis of closed-loop kinematic chains," *IEEE Transactions on Robotics and Automation*, vol. 6, pp. 281-290, 1990.

Appendix 1

$$\tau_2 = -M_1 \sin q_2 + 2L_2(-y_E \cos q_2 + (z_E - z_A)\sin q_2)\cdot$$
$$(2M_3(z_E - z_C - L_3 \cos q_3) + 2M_4(-y_E + L_3 \sin q_3))/A$$
$$\tau_3 = -M_2 \sin q_3 + 2L_3(-y_E \cos q_3 + (z_E - z_C)\sin q_3)\cdot$$
$$(2M_3(-z_E + z_A + L_2 \cos q_2) + 2M_4(y_E - L_2 \sin q_2))/A$$

where

$$A = 4(L_3(-y_E \cos q_3 + (z_E - z_A)\sin q_3) -$$
$$L_2(-y_E \cos q_2 + (z_E - z_C)\sin q_2) + L_2 L_3 \cdot$$
$$\sin(q_2 - q_3) + y_E(z_A - z_C))$$
$$M_1 = g(m_2 r_2 + m_7 L_2 r_7 / L_7)$$
$$M_2 = g(m_3 r_3 + m_8 L_3 r_8 / L_8)$$
$$M_3 = g(m_7(L_7 - r_7)/L_7 + m_8(L_8 - r_8)/L_8 + R_{Ez})$$
$$M_4 = R_{Ey}$$

Appendix 2

$$p_i(t) = a_6 t^6 + a_5 t^5 + a_4 t^4 + a_3 t^3 + a_2 t^2 + a_1 t + a_0$$

with

$$a_0 = b_5,\ a_1 = 2b_7,\ a_2 = -3b_5 + 4b_8,\ a_3 = -4b_7 + 8b_6,$$
$$a_4 = -a_2,\ a_5 = a_1 \text{ and } a_6 = -a_0$$

where

$$b_0 = -\sum_{WS} \tau_i \sin q_i,\ b_1 = \sum_{WS} \tau_i \cos q_i,\ b_2 = \sum_{WS} \sin^2(q_i),$$
$$b_3 = \sum_{WS} \cos^2(q_i),\ b_4 = -2\sum_{WS} \cos q_i \sin q_i$$
$$b_5 = \sum_{WS} (\tau_i b_2 \cos q_i + b_0 \cos q_i \sin q_i),$$
$$b_6 = \sum_{WS} (\tau_i b_3 \sin q_i - b_1 \cos q_i \sin q_i),$$
$$b_7 = \sum_{WS} (\tau_i (b_4 \cos q_i + b_2 \sin q_i) + b_0(\sin^2(q_i) - \cos^2(q_i)) + b_1 \cos q_i \sin q_i)$$
$$b_8 = \sum_{WS} (\tau_i (b_3 \cos q_i + b_4 \sin q_i) + b1_0(\sin^2(q_i) - \cos^2(q_i)) - b_0 \cos q_i \sin q_i)$$

Appendix 3

g = 9.81 m/s², $m_2 = m_4$ = 1.235kg, $m_3 = m_5$ = 1.549kg, m_6 = 0.331kg, $m_7 = m_8 = m_9 = m_{10}$ = 0.536kg, m_{11} = 0.107kg, m_{12} = 0.083kg, m_{13} = 0.111 kg, $L_2 = L_4$ = 0.5m, $L_3 = L_5$ = 0.7m, $L_7 = L_8 = L_9 = L_{10}$ = 0.6m, L_f=0.1m, $z_A = z_F$ = 0.13m, $z_C = z_K$ = 0.28m, $r_2 = r_4$= 0.2094m, $r_3 = r_5$ = 0.3046m, $r_7 = r_8 = r_9 = r_{10}$ = 0.3m, r_{11} = 0.0355m and r_{12} = 0.0315m.